

Dalton Transactions

Accepted Manuscript



This is an *Accepted Manuscript*, which has been through the Royal Society of Chemistry peer review process and has been accepted for publication.

Accepted Manuscripts are published online shortly after acceptance, before technical editing, formatting and proof reading. Using this free service, authors can make their results available to the community, in citable form, before we publish the edited article. We will replace this *Accepted Manuscript* with the edited and formatted *Advance Article* as soon as it is available.

You can find more information about *Accepted Manuscripts* in the [Information for Authors](#).

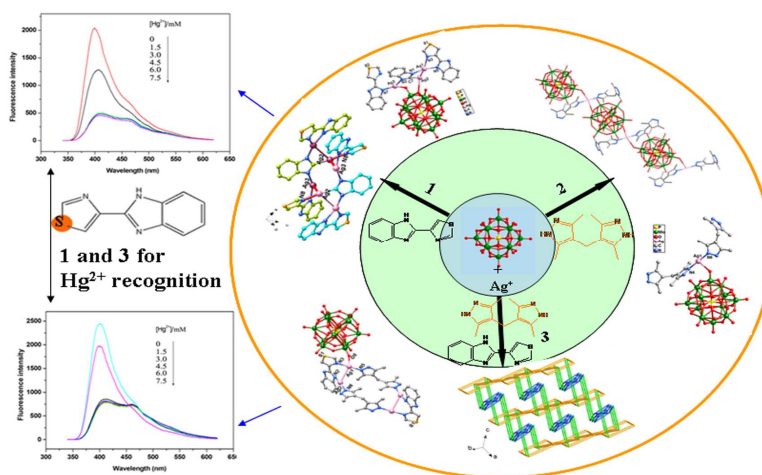
Please note that technical editing may introduce minor changes to the text and/or graphics, which may alter content. The journal's standard [Terms & Conditions](#) and the [Ethical guidelines](#) still apply. In no event shall the Royal Society of Chemistry be held responsible for any errors or omissions in this *Accepted Manuscript* or any consequences arising from the use of any information it contains.

Three new POM-based compounds constructed by rigid thiabendazole and flexible bis(pyrazole) ligands: structures and properties for Hg^{2+} recognition

Aixiang Tian,* Yali Ning, Yang Yang, Xue Hou, Jun Ying, Guocheng Liu, Juwen Zhang, Xiuli Wang*

Department of Chemistry, Bohai University, Jinzhou, 121000, P. R. China

The introduction of S atoms to ligands induces the properties for Hg^{2+} recognition of POM-based compounds.



Cite this: DOI: 10.1039/c0xx00000x

www.rsc.org/xxxxxx

ARTICLE TYPE

Three new POM-based compounds constructed by rigid thiabendazole and flexible bis(pyrazole) ligands: structures and properties for Hg²⁺ recognition†

5 Aixiang Tian,* Yali Ning, Yang Yang, Xue Hou, Jun Ying, Guocheng Liu, Juwen Zhang, Xiuli Wang*

Received (in XXX, XXX) Xth XXXXXXXXXX 20XX, Accepted Xth XXXXXXXXXX 20XX

DOI: 10.1039/b000000x

By using mixed rigid and flexible organic ligands, three Keggin based compounds, [Ag₆(tbz)₄(bmz)₂(H₃PW₁₂O₄₀)]·4H₂O (**1**), [Ag(H₂bdpm)₂(H₂PMo₁₂O₄₀)]·7.5H₂O (**2**), [Ag₄(tbz)₂(H₂bdpm)₂(HPMo₁₂O₄₀)]·2H₂O (**3**) (Htbz = thiabendazole, Hbmz = benzimidazole, H₂bdpm = 1,1'-bis(3,5-dimethyl-1H-pyrazolate)methane), were hydrothermally synthesized and structurally characterized. Through adopting rigid Htbz ligands, compound **1** with hexa-nuclear Ag^I clusters has been obtained. These hexa-nuclear clusters are linked by Keggin anions alternately to form a one dimensional (1D) chain. In compound **2**, the organic moiety is the flexible H₂bdpm ligand. The Keggin anions are fused by [Ag(H₂bdpm)₂]⁺ subunits to form a 1D chain. In compound **3**, the rigid Htbz and flexible H₂bdpm cooperate to modify the anions. Two tbz and two H₂bdpm are fused by four Ag^I ions to construct a tetra-nuclear Ag^I cycle. The anions connect these cycles through Ag-O bonds alternately to form a 1D chain. Adjacent chains arrange parallel to build a 2D layer. The chains in adjacent layers are vertically packing and linked by Ag-O bonds to construct a 3D framework. The electrochemical and photocatalytic properties of the title compounds have been studied. Furthermore, we have also studied the Hg²⁺ recognition properties in suspension of compounds **1** and **3**.

Introduction

Polyoxometalates (POMs), as nano-sized metal oxide clusters, have become appealing inorganic building blocks by virtue of their various structures and conceivable applications.¹ Owing to the abundant terminal and bridging oxygen atoms of POMs, a current research interest is the introduction of transition metal complexes (TMCs) to POMs, which can be grafted onto the framework of POMs *via* covalent bonds and be served as bridging moieties.² In this series, single type of organic ligand was usually chosen, combined with transition metals to modify POMs. However, the introduction of mixed organic molecules to POM-TMCs is relatively rare.³ For example, Cui and co-workers used mixed ligands bipyridine and 1,10-phenanthroline to modify Keggin anions.⁴ Thus, design and syntheses of versatile POM-TMCs containing mixed organic ligands and exploring new properties have become attractive and challenging branch. In this work, we firstly used rigid ligand thiabendazole (Htbz) and flexible ligand 1,1'-bis(3,5-dimethyl-1H-pyrazolate)methane (H₂bdpm) respectively to modify POMs. And then we adopted the above synthetic strategy by using mixed rigid Htbz and

flexible H₂bdpm to cooperatively modify POMs.

As is known, Hg²⁺ is a dangerous and widespread global pollutant, which can cause serious environmental and health problems.⁵ It is necessary and important to seek new methods for detection of Hg²⁺.⁶ Thus, exploration of POM-TMC compounds to detect Hg²⁺ would become a novel and rising branch of POMs. Observed from the reports, complexes with S-containing ligands can usually act as selective fluorescent molecular probe for Hg²⁺.^{5,7} According to Pearson's hard and soft acids and bases theory, soft Hg²⁺ ions (soft acid) can preferentially interact with sulfur (soft base). Thus, the introduction of S-containing ligands to POM-TMC series may construct new materials as fluorescent molecular probe for Hg²⁺. Thus, in this work, we introduce S-containing thiabendazole ligand to POM-Ag system, which is seldom used in POM field.⁸

Fortunately, three compounds, namely [Ag₆(tbz)₄(bmz)₂(H₃PW₁₂O₄₀)]·4H₂O (**1**), [Ag(H₂bdpm)₂(H₂PMo₁₂O₄₀)]·7.5H₂O (**2**), [Ag₄(tbz)₂(H₂bdpm)₂(HPMo₁₂O₄₀)]·2H₂O (**3**) (Htbz = thiabendazole, Hbmz = benzimidazole, H₂bdpm = 1,1'-bis(3,5-dimethyl-1H-pyrazolate)methane) have been obtained. Rigid ligand Htbz was used in **1** as reactant, flexible H₂bdpm was utilized in **2** and mixed Htbz and H₂bdpm were both captured in **3**. Furthermore, experimental data verify that compounds **1** and **3** exhibit Hg²⁺ recognition in suspension, further confirming the

Department of Chemistry, Bohai University, Jinzhou, 121000, P. R. China. Fax: +86-416-3400158; Tel: +86-416-3400158; Email: tian@bhu.edu.cn, wangxiuli@bhu.edu.cn

†Electronic Supplementary Information (ESI) available: IR Spectra, XRD, CV data and additional figures. CCDC 989452–989454. For ESI and crystallographic data in CIF or other electronic format see DOI: 10.1039/b000000x

rationality of selection of S-containing Htbz as organic g, 0.71 mmol) and H₂bdpm (0.04 g, 0.20 mmol) was dissolved in

Table 1. Crystal Data and Structure Refinements for Compounds 1–3.

	1	2	3
formula	C ₅₄ N ₁₆ H ₄₃ Ag ₆ S ₄ PW ₁₂ O ₄₄	C ₂₂ N ₈ H ₄₉ AgPMo ₁₂ O _{47.5}	C ₄₂ N ₁₄ H ₄₉ Ag ₄ S ₂ PMo ₁₂ O ₄₂
Fw	4632.67	2475.81	3099.8
crystal system	triclinic	triclinic	monoclinic
space group	P-1	P-1	P21/c
a (Å)	13.7230(6)	12.8317(6)	14.7828(6)
b (Å)	13.9629(6)	12.8788(6)	18.2643(8)
c (Å)	14.3365(6)	19.4273(9)	14.7157(6)
α (°)	61.8910(10)	80.6810(10)	90
β (°)	82.9930(10)	89.7920(10)	110.3830(10)
γ (°)	63.8760(10)	78.5860(10)	90
V (Å ³)	2162.81(16)	3104.1(3)	3724.4(3)
Z	1	2	2
D _c (g·cm ⁻³)	3.554	2.649	2.763
μ (mm ⁻¹)	17.417	2.764	3.150
F(000)	2077	2212	2946
final R ₁ ^a , wR ₂ ^b [I > 2σ(I)]	0.0493 0.1131	0.0470 0.1328	0.0442 0.1191
final R ₁ ^a , wR ₂ ^b (all data)	0.0666 0.1064	0.0751 0.1205	0.0655 0.1073
GOF on F ²	1.078	1.021	1.037

$$^a R_1 = \sum \|F_o\| - |F_c| / \sum \|F_o\|, \quad ^b wR_2 = \{\sum [w(F_o^2 - F_c^2)^2] / \sum [w(F_o^2)^2]\}^{1/2}$$

molecules.

Experimental Section

Materials and General Methods. All reagents and solvents for syntheses were purchased from Aladdin Industrial Corporation (Shanghai) and were used as received. Elemental analyses (C, H, and N) were performed on a Perkin-Elmer 2400 CHN elemental analyzer (Perkin-Elmer, Shanghai). The IR spectra were obtained on an Alpha Centaur FT/IR spectrometer (Agilent Technologies, America) with KBr pellet in the 400–4000 cm⁻¹ region. Electrochemical measurements were performed with a CHI 440 electrochemical workstation (CH Instruments, Shanghai). A conventional three-electrode system was used. A saturated calomel electrode (SCE) was used as a reference electrode, and a Pt wire as a counter electrode. Chemically bulk-modified carbon-paste electrodes (CPEs) were used as the working electrodes. Fluorescence spectra were recorded at room temperature on a Hitachi F-4500 fluorescence/phosphorescence spectrophotometer. UV-Vis absorption spectra were obtained using a SP-1901 UV-Vis spectrophotometer (Shanghai Spectrum).

Synthesis of [Ag₆(tbz)₄(bmz)₂(H₃PW₁₂O₄₀)]·4H₂O (1). A mixture of H₃[PW₁₂O₄₀]·12H₂O (0.14 g, 0.044 mmol), AgNO₃ (0.20 g, 1.0 mmol) and Htbz (0.04 g, 0.20 mmol) was dissolved in 10 mL of distilled water at room temperature. When the pH of the mixture was adjusted to about 1.8 with 1.0 mol·L⁻¹ HNO₃, the suspension was put into a Teflon-lined autoclave and kept under autogenous pressure at 160°C for 5 days. After slow cooling to room temperature (final pH = 1.9), orange block crystals were filtered and washed with distilled water (30% yield based on W). Anal. Calcd for C₅₄N₁₆H₄₃Ag₆S₄PW₁₂O₄₄ (4632.6): C 13.99, H 0.94, N 4.84%. Found: C 14.05, H 0.96, N 4.88%. IR (solid KBr pellet, cm⁻¹): 3560 (m), 3345 (w), 2915 (w), 1633 (m), 1584 (m), 1514 (m), 1430 (s), 1374 (w), 1329 (w), 1268 (s), 1171 (m), 1066 (s), 965 (s), 877 (s), 798 (s).

Synthesis of [Ag(H₂bdpm)₂(H₂PMo₁₂O₄₀)]·7.5H₂O (2). A mixture of H₃PMo₁₂O₄₀·12H₂O (0.2 g, 0.11 mmol), AgNO₃ (0.12

40 10 mL of distilled water at room temperature. When the pH of the mixture was adjusted to about 1.6 with 1.0 mol·L⁻¹ HNO₃, the suspension was put into a Teflon-lined autoclave and kept under autogenous pressure at 160°C for 5 days. After slow cooling to room temperature (final pH = 1.8), orange block crystals were filtered and washed with distilled water (35% yield based on Mo). Anal. Calcd for C₂₂N₈H₄₉AgPMo₁₂O_{47.5} (2476): C 10.67, H 2.00, N 4.53%. Found: C 10.62, H 1.96, N 4.57%. IR (solid KBr pellet, cm⁻¹): 3447 (m), 3376 (w), 3095 (w), 1628 (m), 1430 (m), 1396 (w), 1325 (w), 1295 (w), 1176 (w), 1067 (s), 970 (s), 886 (s), 803 (s).

Synthesis of [Ag₄(tbz)₂(H₂bdpm)₂(HPMo₁₂O₄₀)]·2H₂O (3). Compound 3 was prepared similarly to compound 2, except that Htbz (0.04 g, 0.20 mmol) was added additionally. After slow cooling to room temperature (final pH = 1.7), orange block crystals were filtered and washed with distilled water (30% yield based on Mo). Anal. Calcd for C₄₂N₁₄H₄₉Ag₄S₂PMo₁₂O₄₂ (3099.8): C 16.27, H 1.59, N 6.33%. Found: C 16.22, H 1.69, N 6.28%. IR (solid KBr pellet, cm⁻¹): 3507 (m), 3349 (m), 3086 (w), 2919 (w), 1619 (m), 1426 (m), 1325 (w), 1272 (w), 1167 (w), 1057 (m), 939 (s), 860 (m), 794 (s).

Preparations of 1–, 2– and 3–CPEs. The compound 1 bulk-modified CPE (1–CPE) was fabricated as follows: 90 mg of graphite powder and 8 mg of 1, were mixed and ground together by an agate mortar and pestle to achieve a uniform mixture, and then was added 0.1 mL of Nujol with stirring. The homogenized mixture was packed into a glass tube with a 1.5 mm inner diameter, and the tube surface was wiped with weighing paper. Electrical contact was established with a copper rod through the back of the electrode. In a similar manner, 2– and 3–CPEs were made with compounds 2 and 3.

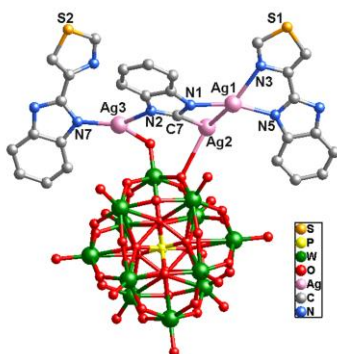
X-ray Crystallographic Study. X-ray diffraction analysis data for compounds 1–3 were collected with a Bruker Smart Apex CCD diffractometer (Bruker Corporation, Germany) with Mo-Kα (λ = 0.71073 Å) at 293 K. The structures were solved by direct methods and refined on F² by full-matrix least squares methods using the SHELXTL package.⁹ For the compounds, all the

hydrogen atoms attached to carbon atoms were generated geometrically, while the hydrogen atoms attached to water molecules were not located but were included in the structure factor calculations. A summary of the crystallographic data and structural determination for them is provided in Table 1. Selected bond lengths and angles of the three compounds are listed in Table S1 (Supporting Information). Crystallographic data for the structures reported in this paper have been deposited in the Cambridge Crystallographic Data Center with CCDC Number 989452 for **1**, 989453 for **2** and 989454 for **3**.

Results and Discussion

Structural description

Crystal Structure of Compound 1. Crystal structure analysis reveals that compound **1** consists of six Ag^{I} ions, four tbz and two bmz ligands, one $[\text{PW}_{12}\text{O}_{40}]^{3-}$ anion (abbreviated to PW_{12}), and four crystal water molecules (Fig. 1). The valence sum calculations¹⁰ show that all the twelve W atoms are in +VI oxidation state (Table S2) and all the Ag atoms are in +I oxidation state. Furthermore, each Hbmz ligand precursor has lost one proton to act as a bmz^- anion (simplified as bmz), and each Htbz ligand precursor has lost one proton to act as a tbz^- anion (simplified as tbz). To balance the charge of the compound, three protons are added, then **1** is formulated as $[\text{Ag}_6(\text{tbz})_4(\text{bmz})_2(\text{H}_3\text{PW}_{12}\text{O}_{40})] \cdot 4\text{H}_2\text{O}$.



25

Fig. 1. Ball/stick view of the asymmetric unit of **1**. The hydrogen atoms and crystal water molecules are omitted for clarity.

In compound **1**, there are three crystallographically independent Ag^{I} ions. The $\text{Ag}1$ ion is four-coordinated by three N atoms from one tbz ligand (N3 and N5) and one bmz ligand (N1) and one $\text{Ag}2$ ion in a slightly distorted quadrilateral-type coordination mode. The bond distances and angles around the $\text{Ag}1$ are 2.105(9)–2.454(11) Å for Ag–N, 3.1452(14) Å for Ag–Ag and 73.0(4)–161.4(4)° for N–Ag–N. The $\text{Ag}2$ ion shows a tetrahedral mode coordinated by one C7 atom from one bmz ligand, one N8 atom from one tbz ligand, one O9 atom from one anion and two Ag^{I} ions ($\text{Ag}1$ and $\text{Ag}3$). The bond distances and angles around the $\text{Ag}2$ are 2.149(9) Å for Ag–N, 2.150(9) Å for Ag–N, 2.9334(14) and 3.1452(14) Å for Ag–Ag and 171.9(4)° for C–Ag–N. The $\text{Ag}3$ ion is four-coordinated by two N atoms from one tbz (N7) and one bmz (N2) ligand, one O7 atom from one anion and one $\text{Ag}2$ ion in a pyramid coordination mode. The Ag–N distances around $\text{Ag}3$ are 2.152(9) and 2.153(9) Å, while the Ag–O distance is 2.763(11) Å. The Ag–C bonds are not very commonly observed in POM–Ag compounds.¹¹

45

In the synthetic process of **1**, the organic ligand Htbz was utilized initially. However, under hydrothermal conditions some Htbz molecules transferred to Hbmz in situ. Thus, there exist two kinds of organic ligands tbz and bmz in compound **1**. The tbz ligands exhibit two types of coordination modes: (i) Two N donors offered by thiazolyl and benzimidazolyl groups play a chelate role to fuse one $\text{Ag}1$ ion (Fig. S1, a-type); (ii) These two N donors also offered by thiazolyl and benzimidazolyl groups link two Ag ions ($\text{Ag}1$ and $\text{Ag}2$) (Fig. S1, b-type). Furthermore, there exhibit strong metal-metal bond between these two Ag ions. This coordination mode is scarcely observed in similar chelate 2,2'-bipy molecules, which may be rest on the longer N...N distance in tbz ligand. The transferred bmz ligand in **1** also shows a novel coordination mode, providing two N donors and the apical C atom to link three Ag ions with Ag–N and Ag–C bonds. Both tbz and bmz ligands exhibit interesting coordination styles.

In compound **1**, two tbz molecules and one bmz are connected by three Ag ions to form a plane (Fig. 1). Furthermore, the same two sets of planes are fused by $\text{Ag}2$ -N8 and $\text{Ag}2$ -Ag3 bonds, as shown in Fig. 2. Thus, a hexa-nuclear Ag^{I} clusters is formed. The Keggin anion offers one terminal O7 and one bridging O9 to link $\text{Ag}3$ and $\text{Ag}2$ ions of this hexa-nuclear clusters and a 1D chain is constructed (Fig. 3). Between adjacent 1D chains there exist abundant $\pi \dots \pi$ stacking interactions ($\text{C}21 \dots \text{C}25 = 3.59$ Å, $\text{C}18 \dots \text{N}6 = 3.82$ Å, $\text{C}23 \dots \text{C}24 = 3.81$ Å) and a 2D supramolecular layer is built (Fig. S2).

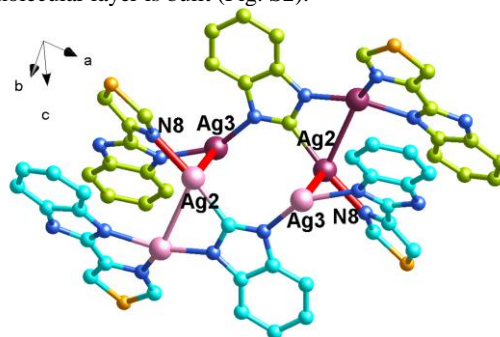


Fig. 2. The hexa-nuclear Ag^{I} clusters in **1** constructed by two sets of planes (yellow and blue) with $\text{Ag}2$ -N8 and $\text{Ag}2$ -Ag3 bonds as linkers (red line).

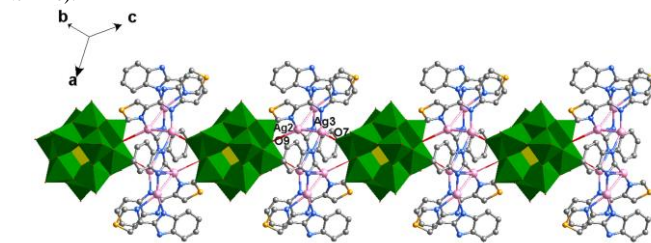


Fig. 3. The hexa-nuclear clusters are linked by Keggin anions alternately to form a 1D chain in compound **1**.

Crystal Structure of Compound 2. Crystal structure analysis reveals that compound **2** consists of one Ag^{I} ions, two H_2bdpm ligands, one $[\text{PMo}_{12}\text{O}_{40}]^{3-}$ anion (abbreviated to PMo_{12}), and seven and a half crystal water molecules (Fig. S3). The valence sum calculations¹⁰ show that all the Mo atoms are in +VI oxidation state (Table S2) and all the Ag atoms are in +I oxidation state. To balance the charge of the compound, two protons are added in the formula of **2**. In compound **2**, there is

only one crystallographically independent Ag^I ion, showing a “seesaw” geometry coordinated with two N donors from two H₂bdpm ligands and two terminal O atoms from two anions. The bond distances and angles around Ag^I are 2.122(6) and 2.134(7) Å for Ag-N, 2.789(6) and 2.798(8) Å for Ag-O and 176.9(3)° for N-Ag-N. Compound **2** shows a 1D chain with PMO₁₂ anions and [Ag(H₂bdpm)₂]⁺ arranging alternately (Fig. 4). The structure is isostructural with compound [Ag(H₂bdpm)₂(H₂PW₁₂O₄₀)]·4H₂O reported by our group.¹²

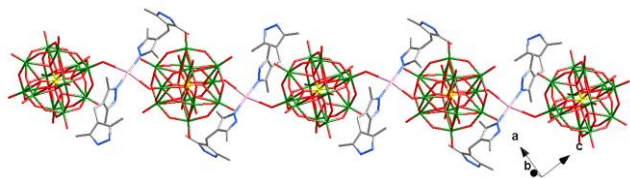


Fig. 4. The 1D chain with PMO₁₂ anions and [Ag(H₂bdpm)₂]⁺ arranging alternately in compound **2**.

Crystal Structure of Compound 3. Crystal structure analysis reveals that compound **3** consists of four Ag^I ions, two H₂bdpm and two tbz ligands, one [PMO₁₂O₄₀]³⁻ anion (abbreviated to PMO₁₂), and two crystal water molecules (Fig. 5). The valence sum calculations¹⁰ show that all the twelve Mo atoms are in +VI oxidation state (Table S2) and all the Ag atoms are in +I oxidation state. Furthermore, each Htbz ligand precursor has also lost one proton to act as a tbz⁻ anion (simplified as tbz), one proton is also added in the formula to balance the charge of the compound **3**.

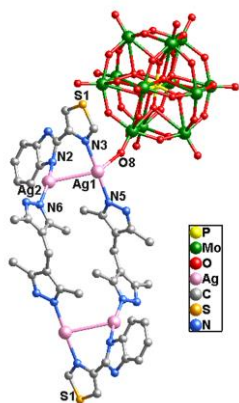


Fig. 5. Ball/stick view of the asymmetric unit of **3**. The hydrogen atoms and crystal water molecules are omitted for clarity.

There are two crystallographically independent Ag^I ions in compound **3**, both exhibiting a “seesaw” geometry coordinated by one Ag ion, one terminal O atom from one PMO₁₂ anion (O8 for Ag^I and O20 for Ag^{II}) and two N donors from one tbz (N3 for Ag^I and N2 for Ag^{II}) and one H₂bdpm (N5 for Ag^I and N6 for Ag^{II}) respectively. The bond distances and angles around the Ag ion are 2.115(6)–2.173(6) Å for Ag-N, 3.2165(10) Å for Ag-Ag, 2.663(6) and 2.744(6) Å for Ag-O and 167.6(3) and 178.6(3)° for N-Ag-N.

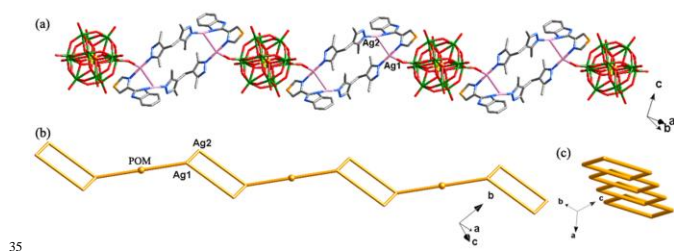


Fig. 6. (a) The 1D chain in compound **3** with anions and tetra-nuclear Ag^I cycles connecting each other alternately. (b) The schematic view of the 1D chain. (c) This 1D chain is viewed along the given direction.

In compound **3**, the mixed flexible H₂bdpm and rigid tbz cooperate to construct the unique structure of **3**. The tbz exhibits the same b-type coordination mode with compound **1** to link two Ag^I ions, by offer two N donors from thiazolyl and benzimidazolyl groups respectively. The H₂bdpm provides two apical N atoms from two pyrazolyl groups to connect two Ag^I ions. The coordination styles of H₂bdpm and tbz induce a tetra-nuclear Ag^I cycle in compound **3** (Fig. 5). The existence of Ag^I-Ag^{II} bonds strengthen the stability of this cycle. Each PMO₁₂ anion supplies two symmetrical terminal O8 atoms to link two tetra-nuclear Ag^I cycles. Namely, the anions and tetra-nuclear Ag^I cycles connect each other alternately and a 1D chain is formed, as shown in Fig. 6. Each chain offers O20 and Ag2 to link adjacent chains through Ag2-O20 bonds. The chain is vertical with its adjacent linking chains (Fig. S4). Through this linking mode, a 3D framework of compound **3** is constructed (Fig. 7).

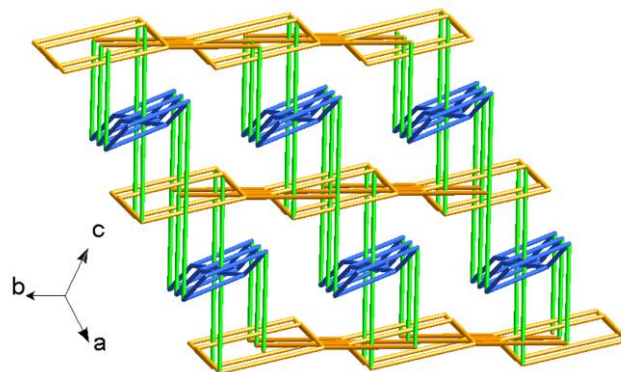
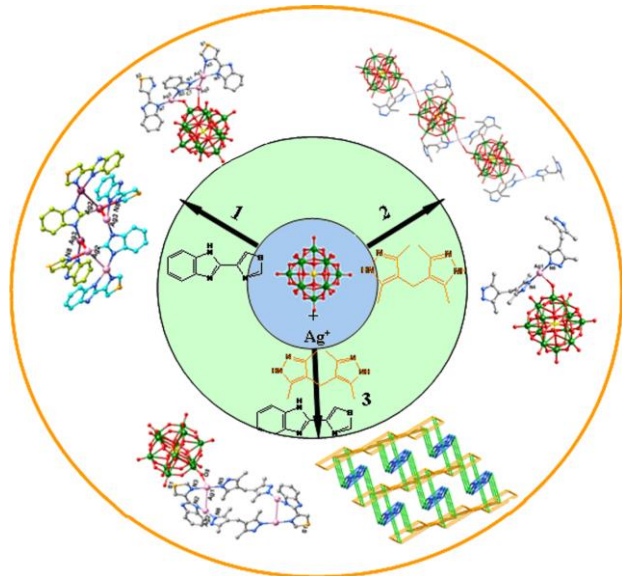


Fig. 7. The 3D framework of compound **3**. Blue and orange sticks: adjacent vertical chains. Green sticks: Ag^{II}-O20 bonds to link adjacent vertical chains.

The respective and cooperative roles of rigid Htbz and flexible H₂bdpm to construct Keggin based structures. In the reported POM-based inorganic-organic compounds, the rigid and flexible organic ligands are usually used to modify POM anions. The rigid and flexible ligands own their unique coordination styles respectively and can induce different POM-based structures. In this work, we choose one rigid ligand thiabendazole (Htbz) and one flexible ligand 1,1'-bis(3,5-dimethyl-1H-pyrazol-5-yl)ethane (H₂bdpm) to construct POM-based compounds respectively and cooperatively (Scheme 1). The rigid Htbz was utilized alone and compound **1** was obtained. Some Htbz molecules transferred to Hbmz in situ under hydrothermal conditions. The coordination characters of tbz and bmz induce a hexa-nuclear Ag^I cluster, which are linked by Keggin anion to form a 1D chain. The single H₂bdpm used in compound **2** only constructs a simple mono-nuclear [Ag(H₂bdpm)₂]⁺ unit, also

connected by anions to build a 1D chain. Furthermore, both Htbz and H₂bdpm were chosen together to construct a novel structure. The mixed tbz and H₂bdpm cooperate to form a tetra-nuclear Ag^I cycle of compound **3**. The anions and cycles arrange alternately to form a 1D chain. Adjacent chains are vertical and linked through Ag²-O20. Thus, a 3D framework is formed. Not only single ligand but also cooperation of Htbz and H₂bdpm can induce new structures of **1–3**.



Scheme 1. The rigid tbz and flexible H₂bdpm to construct Keggin based structures respectively (**1** and **2**) and cooperatively (**3**).

IR spectra. Fig. S5 shows the IR spectra of compounds **1–3**. In the spectrum of **1**, characteristic band at 1066, 965, 877 and 798 cm⁻¹ are attributed to $\nu(\text{P-O})$, $\nu(\text{W-O}_d)$ and $\nu(\text{W-O}_{b/c}\text{-W})$.¹³ In the spectra of **2** and **3**, characteristic bands at 1067, 970, 886 and 803 cm⁻¹ for **2** and 1057, 939, 860 and 794 cm⁻¹ for **3**, are attributed to $\nu(\text{P-O})$, $\nu(\text{Mo-O}_d)$ and $\nu(\text{Mo-O}_{b/c}\text{-Mo})$, respectively.¹⁴ Bands in the regions of 1633–1171 cm⁻¹ for **1**, 1628–1176 cm⁻¹ region for **2**, and 1619–1167 cm⁻¹ for **3** are attributed to the Htbz, Hbmz and H₂bdpm ligands, respectively.

Cyclic voltammetry. Cyclic Voltammetric methods represent a very extensive use method of studying the electrochemical properties of cluster anions. The bulk-modified carbon paste electrode (CPE) has become an optimal choice to study the electrochemical properties for the target compounds, which is credible and inexpensive, easy to prepare and handle.¹⁵ The cyclic voltammograms for **1–** and **3–CPEs** in 0.1 M H₂SO₄ + 0.5M Na₂SO₄ aqueous solution at different scan rates are shown in Fig. 8. For **1–CPE**, two reversible redox peaks can be observed in the potential range of -780 to 0 mV for **1–CPE**. The half-wave potentials $E_{1/2} = (E_{pa} + E_{pc})/2$ are -523 (I-I') and -728 (II-II') mV (scan rate: 100 mV·s⁻¹). The redox couples I-I' and II-II' are ascribed to two consecutive two-electron processes of the PW₁₂.¹⁶ The electrochemical behaviors of the **2–** and **3–CPEs** are similar, and the **3–CPE** has been taken as an example to study their electrochemical properties. In the potential range of -180 to +650 mV, there exist three reversible redox peaks I-I', II-II' and III-III' for **3–CPE** with the half-wave potentials at +284 (I-I'), +100 (II-II'), -122 (III-III') mV (scan rate: 100 mV·s⁻¹), which are ascribed to three consecutive two-electron processes of the

PMO₁₂.¹⁷ When the scan rates varied from 20 to 300 mV·s⁻¹ for **1–** and **3–CPE**, the peak potentials change gradually; the cathodic peak potentials shift towards the negative direction, while the corresponding anodic peak potentials to the positive direction. The peak currents are proportional to the scan rates up to 300 mV·s⁻¹ (Fig. S6), which indicate that the redox process of the **1–** and **3–CPEs** are surface-confined.

Fig. S7 shows cyclic voltammograms for the electrocatalytic reduction of hydrogen peroxide by the **1–** and **3–CPE** in 0.1 M H₂SO₄ + 0.5M Na₂SO₄ aqueous solution. For **1–CPE**, it can be clearly seen that with addition of hydrogen peroxide, both two reduction peak currents gradually increase while the corresponding oxidation peak currents decrease, suggesting that **1–CPE** shows good electrocatalytic activity toward the reduction of H₂O₂. However, for **3–CPE**, with addition of hydrogen peroxide the second and the third reduction peak currents gradually increase while the corresponding oxidation peak currents decrease, but the first redox peak remains almost unchanged, which indicates that the four- and six-electron reduced species of PMO₁₂ anions present electrocatalytic activity at **3–CPE** for the reduction of hydrogen peroxide. Obviously, the third reduced species show the best electrocatalytic activity, namely, the catalytic activity is enhanced with increasing extent of POM anion reduction.

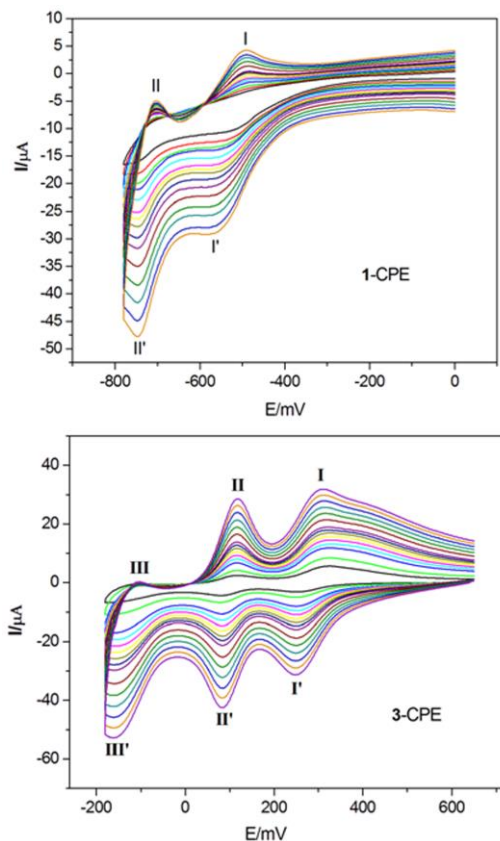


Fig. 8. The cyclic voltammograms of the **1–** and **3–CPEs** in 0.1 M H₂SO₄ + 0.5M Na₂SO₄ at different scan rates (from inner to outer: 20, 40, 60, 80, 100, 120, 140, 160, 180, 200, 220, 240, 260, 280 and 300 mV·s⁻¹).

Photocatalytic activity. The photocatalytic activities of compounds **1–3** were studied by the degradation of methylene blue (MB) solution under UV irradiation. In the process of photocatalysis, 100 mg compounds was suspended in 0.02

mmol/L MB aqueous solution 250 mL and magnetically stirred for about 10 min to ensure the equilibrium in the dark. Then 5.0 mL samples were taken out every 20 min for analysis by UV-visible spectroscopy. However, the absorption peaks of MB with compound **2** show almost no obvious change. It can be clearly observed from Fig. 9 and Fig. S8 that the absorption peaks of MB photocatalyzed by **1** decreased obviously with increasing of reaction time and the conversions of MB is 89.1% after 140 min. The conversion of MB photocatalyzed by **3** is the lower with 40.5%, which maybe rest on the different polyoxomolybdate anions. This results show that compounds **1** and **3** own excellent photocatalytic activities for the degradation of MB, especially **1**.

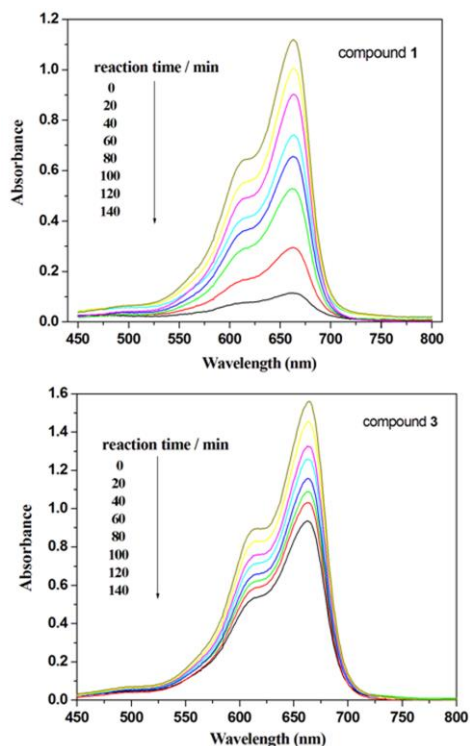


Fig. 9. Absorption spectra of the MB solution during the decomposition reaction under UV irradiation with the presence of compounds **1** and **3**.

Luminescent sensing functions to Hg^{2+} of compounds **1** and **3**.

At present, some coordination polymers containing sulfur atoms as a mercury-coordinating element have usually been used as highly selective luminescent probes for Hg^{2+} .^{5,7} In this work, we design compounds **1** and **3** employing S-based Htbz to explore the potential sensing functions of Hg^{2+} in suspension of distilled water of **1** and **3**. The emission spectrum of **1** suspension at room temperature excited at 320 nm shows an intense emission band at 399 nm (Fig. 10a). When addition Hg^{2+} to compound **1** suspension, its luminescence quenched three-quarter until the concentration of Hg^{2+} was enhanced higher than 4.5 mM. Furthermore, in order to make a further understanding of this phenomenon, we have performed the same experiments to introduce Ag^+ , Zn^{2+} , Cd^{2+} , Pb^{2+} , Cu^{2+} and Fe^{3+} to the system. With addition of 4.5 mM Zn^{2+} , Cd^{2+} , Pb^{2+} and Fe^{3+} to the suspension of **1** respectively, the luminescent intensities increase (Fig. 10b). Although the introduction of Ag^+ , Cu^{2+} can also decrease the luminescent intensities, the decreasing degree is not obvious compared with Hg^{2+} .

The same phenomenon happened on compound **3**. Namely, the introduction of Hg^{2+} decreased the luminescent intensities of **3**, and with enhancing the Hg^{2+} concentration up to 4.5 mM, the luminescent intensities change to the lowest level (Fig. 11a). The introduction of Zn^{2+} causes the luminescent intensities of **3** to be enhanced extremely. Although the luminescent intensities decrease by introduction of other equal Ag^+ , Cd^{2+} , Pb^{2+} , Cu^{2+} and Fe^{3+} , the luminescent intensities are still much stronger than that of Hg^{2+} (Fig. 11b).

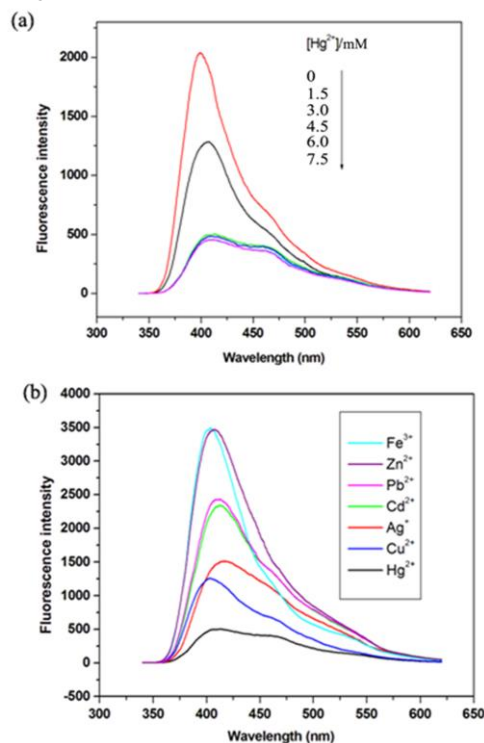


Fig. 10. (a) Emission spectra of **1** suspension in distilled water in the absence and presence of Hg^{2+} with different concentrations (excited at 320 nm). (b) Emission spectra of **1** suspension with addition of different metal ions (4.5 mM, excited at 320 nm).

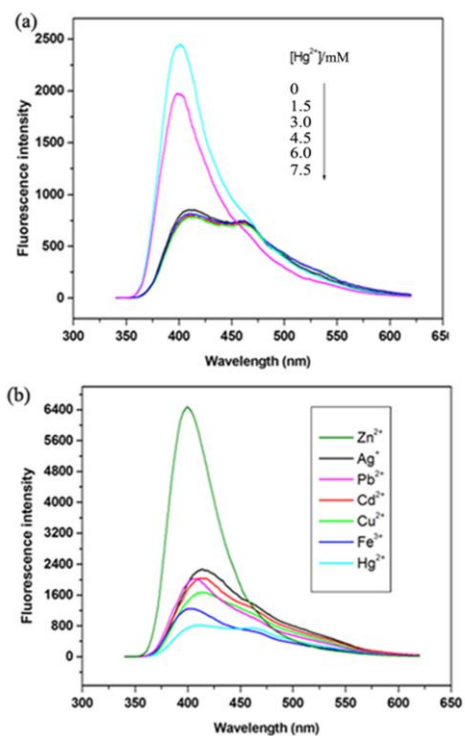


Fig. 11. (a) Emission spectra of **3** suspension in distilled water in the absence and presence of Hg^{2+} with different concentrations (excited at 320 nm). (b) Emission spectra of **3** suspension with addition of different metal ions (4.5 mM, excited at 320 nm).

As shown in Fig. 12, the introductions of Zn^{2+} , Cd^{2+} in **1** suspension and Zn^{2+} in **3** suspension induce the luminescent intensities increase as discussed above. However, when the equal Hg^{2+} was added consequently, the luminescent intensities still decrease, which shows that compounds **1** and **3** acting as fluorescent molecular probes own high selectivities. Furthermore, the luminescent change induced by Fe^{3+} ions in **1** and **3** suspensions respectively is the most distinct, enhancing in **1** suspension and decreasing in **3** suspension obviously. This phenomenon maybe depend on the N-H groups of compound **3**. According to Pearson's hard and soft acids and bases theory, the N-H group is hard base, which is easy to coordinate with Fe^{3+} (hard acid).

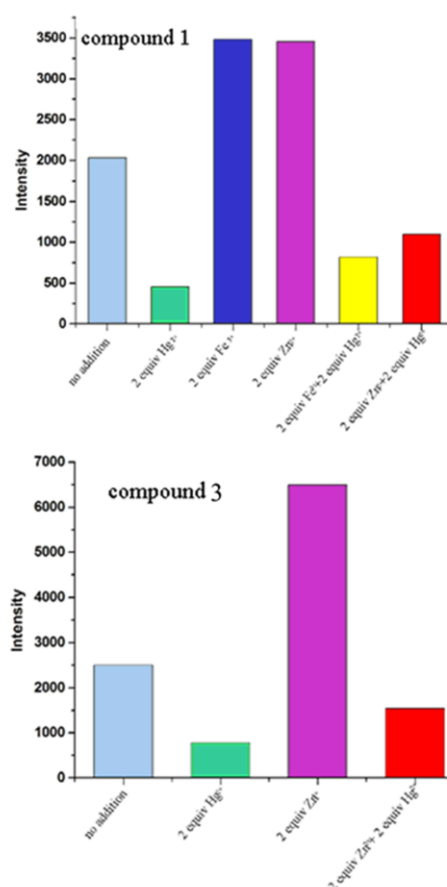


Fig. 12. Luminescent intensity of compounds **1** and **3** at about 399 nm in suspension at room temperature upon the addition of Hg^{2+} , Zn^{2+} or Fe^{3+} ions (excited at 320 nm).

Conclusions

In this work, by using mixed rigid ligand Htbz and flexible ligand H_2bdpm , we have synthesized three POM-based compounds **1–3** under hydrothermal conditions. Compounds **1** and **2** show 1D chain by using rigid Htbz and flexible H_2bdpm , respectively. In compound **3**, mixed Htbz and H_2bdpm are both captured to construct a 3D framework of **3**. The S atoms in **1** and **3** are both non-coordinated and exposed. Compounds **1** and **3** exhibit good luminescent recognition for Hg^{2+} in suspension. Further endeavors will focus on other POM-based Hg^{2+} fluorescent probes by using S-containing ligands.

Acknowledgements

Financial supports of this research by the National Natural Science Foundation of China (No. 21101015, 21471021 and 21201021, 21401010) and Talent-supporting Program Foundation of Education Office of Liaoning Province (LJQ2012097).

Notes and references

- (a) J. Zhou, J. W. Zhao, Q. Wei, J. Zhang, G. Y. Yang, *J. Am. Chem. Soc.* 2014, **136**, 5065; (b) P. Huang, C. Qin, Z. M. Su, Y. Xing, X. L. Wang, K. Z. Shao, Y. Q. Lan, E. B. Wang, *J. Am. Chem. Soc.* 2012, **134**, 14004; (c) S. J. Li, S. M. Liu, S. X. Liu, Y. W. Liu, Q. Tang, Z. Shi, S. X. Ouyang, J. H. Ye, *J. Am. Chem. Soc.* 2012, **134**, 19716; (d)

- S. Ogo, N. Shimizu, K. Nishiki, N. Yasuda, T. Mizuta, T. Sano, M. Sadakane, *Inorg. Chem.* 2014, **53**, 3526.
- 2 (a) S. T. Zheng, J. Zhang, X. X. Li, W. H. Fang, G. Y. Yang, *J. Am. Chem. Soc.* 2010, **132**, 15102; (b) H. J. Pang, J. Peng, C. J. Zhang, Y. G. Li, P. P. Zhang, H. Y. Ma, Z. M. Su, *Chem. Commun.* 2010, **46**, 5097; (c) X. L. Wang, H. L. Hu, G. C. Liu, H. Y. Lin, A. X. Tian, *Chem. Commun.* 2010, **46**, 6485.
- 3 (a) A. Dolbecq, P. Mialane, F. Sécheresse, B. Keita, L. Nadjo, *Chem. Commun.* 2012, **48**, 8299; (b) H. Jin, X. L. Wang, Y. F. Qi, E. B. Wang, *Inorg. Chim. Acta* 2007, **360**, 3347; (c) Z. K. Qu, K. Yu, Z. F. Zhao, Z. H. Su, J. Q. Sha, C. M. Wang, B. B. Zhou, *Dalton Trans.* 2014, **43**, 6744.
- 4 L. M. Wang, Y. Wang, Y. Fan, L. N. Xiao, Y. Y. Hu, Z. M. Gao, D. F. Zheng, X. B. Cui, J. Q. Xu, *CrystEngComm.* 2014, **16**, 430.
- 15 5 Q. Zhao, T. Y. Cao, F. Y. Li, X. H. Li, H. Jing, T. Yi, C. H. Huang, *Organometallics*, 2007, **26**, 2077.
- 6 (a) H. Yang, Z. G. Zhou, K. W. Huang, M. X. Yu, F. Y. Li, T. Yi, C. H. Huang, *Org. Lett.* 2007, **9**, 4729; (b) Z. H. Cheng, G. Li, N. Zhang, H. O. Liu, *Dalton Trans.* 2014, **43**, 4762.
- 20 7 Y. Liu, M. Y. Li, Q. Zhao, H. Z. Wu, K. W. Huang, F. Y. Li, *Inorg. Chem.* 2011, **50**, 5969.
- 8 A. X. Tian, Y. Yang, N. Sun, J. C. Li, J. Ying, J. W. Zhang, X. L. Wang, X. L. J. Coord. Chem. 2014, **67**, 1550.
- 9 G. M. Sheldrick, *SHELXS-97*, University of Göttingen, Germany, 1997.
- 25 10 I. D. Brown, D. Altermatt, *Acta Crystallogr. B.* 1985, **41**, 244.
- 11 (a) M. X. Liang, C. Z. Ruan, D. Sun, X. J. Kong, Y. P. Ren, L. S. Long, R. B. Huang, L. S. Zheng, *Inorg. Chem.* 2014, **53**, 897; (b) P. P. Zhang, J. Peng, H. J. Pang, J. Q. Sha, M. Zhu, D. D. Wang, M. G. Liu, Z. M. Su, *Cryst. Growth Des.* 2011, **11**, 2736.
- 30 12 A. X. Tian, Y. Yang, J. Ying, N. Li, X. L. Lin, J. W. Zhang, X. L. Wang, *Dalton Trans.* 2014, **43**, 8405.
- 13 L. L. Fan, D. R. Xiao, E. B. Wang, Y. G. Li, Z. M. Su, X. L. Wang, J. Liu, *Cryst. Growth Des.* 2007, **7**, 592.
- 14 J. Q. Sha, M. T. Li, J. W. Sun, Y. N. Zhang, P. F. Yan, G. M. Li, *Dalton Trans.* 2013, **42**, 7803.
- 35 15 (a) H. Beitollahi, I. Sheikhshoae, *Electrochim. Acta*, 2011, **56**, 10259; (b) H. Beitollahi, A. Mohadesi, S. Mohammadi, A. Akbari, *Electrochim. Acta*, 2012, **68**, 220; (c) H. Beitollahi, I. Sheikhshoae, *J. Electroanal. Chem.* 2011, **661**, 336; (d) H. Beitollahi, M. Mostafavi, *Electroanalysis*, 2014, **26**, 1090; (e) H. Beitollahi, I. Sheikhshoae, *Anal. Methods*, 2011, **3**, 1810; (f) E. Molaakbari, A. Mostafavi, H. Beitollahi, R. Alizadeh, *Analyst*, 2014, **139**, 4356.
- 40 16 (a) M. Sadakane, E. Steckhan, *Chem. Rev.* 1998, **98**, 219; (b) S. X. Guo, A. W. A. Mariotti, C. Schlipf, A. M. Bond, A. G. Wedd, *Inorg. Chem.* 2006, **45**, 8563.
- 45 17 W. B. Song, Y. Liu, N. Lu, H. D. Xu, C. Q. Sun, *Electrochim. Acta* 2000, **45**, 1639.